AD-A176 753 DEVELOPMENT OF JOSEPHSON JUNCTIONS AND ARRAYS AS INFRARED DETECTORS FOR AN IMAGE PROCESSOR(U) HYPRES INC ELMSFORD NY S BALIGA ET AL. 29 JAN 87 N00014-86-C-0010 1/1

UNCLASSIFIED F/G 17/5 NL

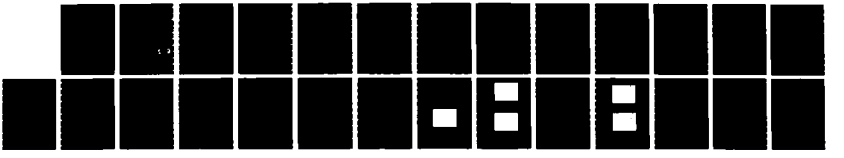

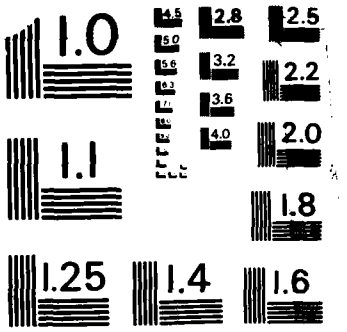

MICROCOPY RESOLUTION TEST CHART

NATIONAL BUREAU OF STANDARDS - 1963 - A

(12)

SECURITY CLASSIFICATION OF THIS PAGE (When Data Entered)

REPORT DOCUMENTATION PAGE	READ INSTRUCTIONS BEFORE COMPLETING FORM
1. REPORT NUMBER	2. GOVT ACCESSION NO. 3 RECIPIENT'S CATALOG NUMBER
4. TITLE (and Subtitle) Development of Josephson Junctions as Infrared Detectors for an Image Processor	5. TYPE OF REPORT & PERIOD COVERED Final Report Nov. 18, 1985 - Dec. 31, 1986
	6. PERFORMING ORG. REPORT NUMBER
7. AUTHOR(s) S. Baliga, M. Radparvar, and S. M. Faris	8. CONTRACT OR GRANT NUMBER(s) Office of Naval Research Contract N00014-86-C-0010
9. PERFORMING ORGANIZATION NAME AND ADDRESS HYPRES, Inc. 500 Executive Boulevard Elmsford, N. Y. 10523	10. PROGRAM ELEMENT, PROJECT, TASK AREA & WORK UNIT NUMBERS
11. CONTROLLING OFFICE NAME AND ADDRESS Department of the Navy, Office of Naval Research, 800 North Quincy Street Arlington, VA. 22217	12. REPORT DATE January 29, 1987
	13. NUMBER OF PAGES 21
14. MONITORING AGENCY NAME & ADDRESS(if different from Controlling Office)	15. SECURITY CLASS. (of this report) Unclassified
	15a. DECLASSIFICATION/DOWNGRADING SCHEDULE

16. DISTRIBUTION STATEMENT (of this Report)

Distribution in accordance with enclosure number one (1)

DISTRIBUTION STATEMENT A
Approved for public release
Distribution Unlimited

17. DISTRIBUTION STATEMENT (of the abstract entered in Block 20, if different from Report)

18. SUPPLEMENTARY NOTES

DTIC ELECTE FEB 17 1987 S D

19. KEY WORDS (Continue on reverse side if necessary and identify by block number)

Superconducting, image processing, Josephson junction, infrared detection, cryogenics

20. ABSTRACT (Continue on reverse side if necessary and identify by block number)

The optical response of Nb-AlOx-Nb Josephson junctions and series arrays of such junctions has been studied in the 1 to 20 micron region of the infrared. Gap suppression on irradiation has been observed, leading to ultra-high sensitivities of order of 10^5 Volt/Watt. Such high responsivities are not possible over an entire wavelength range using conventional technologies. The devices are found to show linear re-

DD FORM 1 JAN 73 1473 EDITION OF 1 NOV 65 IS OBSOLETE

SECURITY CLASSIFICATION OF THIS PAGE (When Data Entered)

sponse even at ultra-low intensities of order 200 femtoWatts/ device. Attempts have been made to further improve the external quantum efficiency and voltage responsivity of the devices by using counterelectrodes with lower reflectivities. The high quantum efficiencies (≳100) of the devices may be explained by the creation of quasi-particles by the incident photon, and a further increase in quasi-particle number density by interaction with phonons.

DEVELOPMENT OF JOSEPHSON JUNCTIONS AND ARRAYS AS INFRARED DETECTORS FOR AN IMAGE PROCESSOR

BY:

S. Baliga, M. Radparvar, and
S.M. Faris
HYPRES, Inc.

January 29, 1987

ABSTRACT

The optical response of Nb-AlOx-Nb Josephson junctions and series arrays of such junctions has been studied in the 1 to 20 micron region of the infrared. Gap suppression on irradiation has been observed, leading to ultra-high sensitivities of order of 10^5 Volt/Watt. Such high responsivities are not possible over an entire wavelength range using conventional technologies. The devices are found to show linear response even at ultra-low intensities of order 200 femtoWatts/device. Attempts have been made to further improve the external quantum efficiency and voltage responsivity of the devices by using counterelectrodes with lower reflectivities. The high quantum efficiencies ($\gtrsim 100$) of the devices may be explained by the creation of quasi-particles by the incident photon, and a further increase in quasi-particle number density by interaction with phonons.

INTRODUCTION

Infrared imaging systems currently in use suffer from problems in the fields of surveillance, data acquisition and discrimination. Currently available conventional technology does not provide high enough sensor responsivity in any but narrow regions of the electromagnetic spectrum.[1] The semiconductor technologies also require a crystalline substrate, and wafer scale integration of both sensors and processing circuits is not always possible. The problems of packaging, reliability, size, weight and cost are compounded by these drawbacks.

New and innovative sensor technology, with high sensitivities from radar to gamma ray regions, is badly needed. Superconducting technology, which does not suffer from the drawbacks of the conventional semiconducting technology is a strong front-runner candidate.

Specifically the useful properties of superconducting elements with reference to their utilization as radiation sensors are:

1) Extremely high sensitivity over the one to twenty micron wavelength range as demonstrated by us in this report.

2) Extendability of this high sensitivity from the microwave region all the way to the gamma ray region.

3) Ultra-high speed of the devices and extremely low power dissipation.

4) Wafer scale integrability of both sensors and processing circuits in superconducting technology.

The ultra-high responsivities of these "cryo-optical" detectors when combined with other features typical to superconducting technology make the detectors extremely attractive as sensors in infrared imaging systems. Some of these features are high speed, low power dissipation, dispersionless transmission lines below gap frequencies (§700 GHz) and last but not least wafer integrability. Integrating, on the same substrate, the imaging arrays with complex digital, as well as analog, processing circuits, will lead to an ultra-high performance imaging system not possible with conventional technologies.

EXPERIMENTAL SETUP

The junction and array samples were conductively cooled in a Heli-Tran, which is a liquid helium transfer refrigeration system. The I-V characteristics and the voltage shifts produced on irradiation were measured using the four-probe method.

Infrared radiation was obtained from a 1000 Watt xenon arc lamp by use of narrow band filters. The radiation entered the Heli-Tran through a silicon anti-reflection coated window which served as a longpass filter permitting all the infrared radiation. Figure 1 shows the block diagram of the experimental setup.

The radiation reaching the sample was uniform in intensity over a region of about 2 cm^2. A small hole in the radiation shield of the Heli-Tran permitted the radiation to fall onto the device under study. The device was thus illuminated with radiation uniformly over its area. Infrared irradiance at the sample position was measured by means of a pyroelectric radiometer. The irradiance varied with the use of different filters from a maximum of about 0.1 W/cm^2 at 1 um to a minimum of about 0.0002 W/cm^2 at the longer wavelengths. Ultra-low intensities of order 1 uW/cm^2 (or 200 femtoWatts/device) were obtained by the use of neutral density filters.

The sample temperature was measured by means of a Germanium Resistance Thermometer (GRT) mounted on the sample holder. Close tracking of the sample temperature was achieved by placing the GRT as close as possible to the chip. The Josephson junctions and arrays are themselves a fairly good thermometer since the value of the gap of a superconductor is a function of temperature.

Care was taken to ensure that the sample temperature was as close to 4.2 K (liquid helium temperature) as possible. This is because at higher temperatures the gap of niobium varies strongly with temperature (dropping to zero at its critical temperature of 9.3 K). At lower temperatures, the optical effects of radiation can be studied without interference from the effects of thermal heating on the energy gap.

The devices were high quality Nb-AlOx-Nb Josephson tunnel junctions. A trilayer composing of niobium/thermally oxidized aluminum/niobium is fabricated, in situ, in a DC magnetron system. Devices are fabricated using Selective Niobium Anodization Process or its modified version[2]. The trilayer is patterned using the first electrode mask and subsequently anodized after patterning with the second mask (junction definition mask). In devices with normal counterelectrode thickness, a deposition and patterning of 3000 Å niobium as wiring channel completes the device fabrication. For devices with thin counterelectrodes, a double layer of aluminum and niobium provides the wiring channel. Aluminum is used as an etch stop when holes are to be etched on top of the junctions into the wiring channel. The aluminum thickness is thin enough (100 Å) to make it superconducting by proximity effect. In addition, the excessive aluminum is removed in the junction area, thus exposing the counterelectrode directly to the incident radiation. In addition, to improve device sensitivity by reducing the reflectivity, junctions were covered with dielectrics such as SiO_2 and anodized niobium, or superconducting NbN was used as the wiring channels. Figure 2 shows part of a chain of 500 Josephson junctions used in the experiments.

EXPERIMENTAL RESULTS

Figure 3 shows the I-V characteristics of a typical Nb-AlOx-Nb junction and Figure 4 the I-V characteristics of an array of 50 junctions in series.

Both single junctions and junctions in arrays were fabricated so that the quasi-particle current density at the sum of the gaps was about 2000 A/cm^2. The single junctions varied in area from 30 * 30 um^2 to 2.5 * 2.5 um^2, while the junctions for arrays were no larger than 10 * 10 um^2. Both fused quartz and silicon were used as substrates. Arrays of size 20, 50 and 500 were fabricated.

Studies of the voltage responsivity of junctions showed a responsivity between 10^4 V/W and 10^5 V/W for high current density devices. Low current density (25 A/cm^2) devices typically had a response of an order of magnitude less. Further experiments on junctions were therefore restricted to high current density devices.

Following Owen and Scalapino's[3] pair-breaking model, the suppression of the gap by quasi-particle creation is given by

$$\Delta/\Delta_o \simeq 1-2n \qquad (1)$$

for small n, where n is the excess quasi-particle number in units of $4N(o)\Delta o$. N(o) is the single-spin density of states and Δo the unperturbed energy gap at T=O K.

The voltage responsivity of junctions of different areas was measured to find a relation between responsivity and area. In accordance with Eq. 1, it was experimentally observed that the gap suppression on light irradiation is independent of area. The voltage responsivity R of a junction is defined as

$$R = \frac{\delta V}{P.A} \qquad (2)$$

where δV is the voltage (gap) shift
P is the incident optical power in W/cm^2
A is the device area in cm^2.

From Eq. 2, it is evident that a larger junction will have a smaller value of voltage responsivity R, than a smaller junction, if both are irradiated with the same optical power. In other words R is inversely proportional to A, and R.A is a constant for junctions which are identical otherwise (same counterelectrode, barrier material and current density, etc.).

Figure 5 shows the variation of voltage responsivity R versus junction area A, for junctions on the same substrate. An inverse relation is evident.

The fact that smaller devices have higher responsivity implies that we can build a very sensitive array using such small junctions in series. Since the gap suppression is independent of area it is not necessary to use large junctions, where optical resolution is sacrified. This gives Josephson detectors an extra edge over semiconducting optical detectors.

Figure 6 shows the I-V characteristics of a single junction with and without irradiation. Figure 7 shows the I-V characteristics of a chain of 50 junctions with and without irradiation. The voltage shifts caused by gap suppression are found as expected to be additive in a series array of junctions. By having the junctions in a series array, weak signals as low as 5 nV per junction can thus be measured since the array "amplifies" the signal.

The product R.A. is a normalized device responsivity since it is independent of area. To compare the performance of different types of Josephson junctions (different electrodes, barrier material, current density etc.) the product R.A. is to be compared and optimized. It may also be pointed out that larger junctions are desirable in an application where high current sensitivity is required. Since the "knee" current of a large junction is greater, bigger current swings on a load line can be obtained with a larger junction.

Figure 8 shows the ultra-high responsivity of 5 * 5 um^2 junctions in a series array of 50. The increased responsivity at the longer wavelengths may be noted and is expected to continue till the 100 micron region and beyond. The junctions and arrays are therefore extremely useful as wideband detectors.

Linearity of response

The linearity of gap suppression versus incident infrared intensity was tested at high (100 mW/cm^2), low (100 uw/cm^2) and ultra low (1uW/cm^2) intensities at 1 um wavelength. For the ultra low intensities, the radiation incident on a 5 * 5 um^2 junction was of the vaule of 100 femtoWatts. This corresponds to a flux of only about 10^6 photons per second per junction and produced a voltage shift of about 5 nanovolts.

The voltage shift was found to vary linearily with intensity in all the three regimes of intensity. Figure 9 shows the voltage shift in an array of 50 junctions, when the radiation intensity at 1 um is varied using a set of neutral density filters. The absolute value of the ultra-low radiation intensity is not measured accurately; only the relative decrease in intensity produced by the insertion of neutral density filters is required in showing linearity. The linearity of the devices at ultra-low intensities is demonstrated.

The signal voltages were measured using a lock-in amplifier and an optical chopper. Shielded cables were used to reduce extraneous noise. Attempts are ongoing to further reduce the noise from its present value of about 10 $nV/\sqrt{Hz}$, to reduce the Noise Equivalent Power (N.E.P.) and optimize system performance. Reduction of the noise will enable more accurate measurement of nanovolt signals in the study of device linearity.

The observed linearity of the devices is expected from theoretical considerations. The number of quasi-particles created is given in steady state by[3]

$$n = rPt/4N(0)V\Delta_o \qquad (3)$$

where V is the volume of illuminated superconductor
r is the number of quasi-particles produced per photon
P is the incident photons per second
t is an effective recombination time.

Combining Eq.1 and Eq.3, we see that the voltage shift is linearily related to the number of incident photons.

System Performance

A test system was implemented to measure small signal voltages and to obtain useful parameters such as Noise Equivalent Power (N.E.P.), Detectivity (D) and Specific Detectivity (D^*).

Figure 1 shows the block diagram of the experimental setup. A lock-in amplifier and high input impedance preamplifier were used in conjunction with an optical chopper. The chopper frequency was varied from 10 HZ to 4 KHZ.

The noise density was measured at low frequencies and found to be about 10 $nV/\sqrt{Hz}$. This was a lock-in limited value, with the detector facing a 300 K background, with a field of view of half-angle about 15 degrees. Immersion in superfluid helium in an optical cryostat and use of an input transformer is planned for future experiments, to reduce the noise level to 1 $nV/\sqrt{Hz}$ or less.

The N.E.P. is given by

$$\text{N.E.P.} = \frac{\text{Noise Density}}{\text{Responsivity}} \qquad (4)$$

For a junction with responsivity of 60,000 V/W the N.E.P. is calculated to be $1.5 * 10^{-13}$ Watts and the D* value to be $7 * 109$ $cm\sqrt{Hz}/Watt$.

Table I compares the present and ultimate N.E.P. of the Josephson detector versus detectors based on other technologies. The system N.E.P. is presently limited by extraneous noise. By further reduction in the noise, the N.E.P. valve can be improved to reach the 1/f limited value of about 10-16 Watts.

Quantum Efficiency

The intrinsic quantum efficiency of a sensor is defined as the number of charge carriers produced per photon entering the sensor material. The external quantum efficiency is the number of charge carriers produced per photon incident on the sensor surface.

Since metallic niobium has a reflectivity of about 80% in the 1 um region[4], the external quantum efficency is about a factor of 5 less than the junction's intrinsic quantum efficiency.

The intrinsic quantum efficency of a niobium Josephson junction may be evaluated as follows. Since a 1 um photon has an energy about 480 times the gap energy of niobium (2.6 mV), each photon entering the counterelectrode is capable of breaking at most 480 pairs. This gives rise to 960 quasi-particles, which are the charge carriers.

Though the incident photon does not break 480 pairs, the high energy quasi-particles produced by the incident photon, interact with phonons and Cooper pairs to further produce more quasi-particles, in an "avalanche" of quasi-particle production.

Since only 20% of the light incident on the counterelectrode leads to quasi-particle creation, the external quantum efficency should at best be 20% of 960 = 190. From the experimental data, the observed quantum efficiency is about 100 for niobium devices. This is only an estimate based on approximations of the optical penetration depth and uniform quasi-particle density.

Table 1 also lists the external quantum efficiencies of some detectors based on different technologies. Typically, the quantum efficiencies are less than 1 (or 100%). Only the avalanche type detectors have quantum efficiencies comparable to the Josephson detector.

The external quantum efficiency may be further improved by use of a coating or layer which has a lower reflectivity than niobium, on the counterelectrode. The theory in this case is more complicated since quasi-particles may be produced in this layer, if it is superconducting. Increased light absorption is observed as a stronger gap suppression and increased responsivity.

Layers of silicon dioxide (SiO_2) and niobium oxide (Nb_2O_5), which are weakly reflecting did not much improve device responsivity. However, use of superconducting niobium nitride (NbN) as the metallization layer for the junction has lead to a doubling of gap suppression, voltage responsivity and quantum efficiency. The increase of quantum efficiency to 200 (Table 1) from 100 is expected since the reflectivity of niobium nitride is close to 60% at 1 um (as measured by us).

With present technology, high quality and high current density niobium nitride junctions are not yet available[5], so it was not possible to explore the use of niobium nitride junctions as infrared sensors. Further experiments are therefore planned with niobium nitride metallizations to optimize junction and array performance.

CONCLUSION AND FUTURE WORK

In summary, niobium based Josephson junctions and arrays of such junctions have shown ultra-high sensitivity to infrared radiation in the entire 1 to 20 micron region. The response has been highest approaching 10^5 Volt/Watt for junctions with high current density. The responsivity has been studied with respect to such parameters as light intensity, wavelength and junction area. Linearity of the response has been demonstrated with intensities as low as 200 femtowatts/device. High quantum efficiencies (§100) of the devices may be explained by the creation of quasi-particles by the incident high-energy photon, with a further increase in quasi-particle number by interactions with phonons. Attempts are ongoing to further improve the quantum efficiency and voltage responsivity of the devices by the use of counterelectrodes having lower reflectivity.

Future work on the development of the infrared image processing system based on Josephson technology, is planned in two phases. In Phase II device response and system performance in the 1 to 20 micron wavelength region will be further optimized. The concept of peripheral circuitry will be explored. A 2 x 2 array will be fabricated and tested, and extendability to larger arrays for imaging demonstrated.

In Phase III a complete prototype image processing system including peripheral circuitry and cooling subsystems such as closed-cycle refrigerators will be developed. This phase will provide wafer-scale integration that incorporates sensor arrays with analog and digital processing circuits. The array performance will be extended to the 100 micron region using a far-infrared laser. This will result in an image processing system with extremely wide bandwidths not possible with conventional technologies.

REFERENCES

1) John A. Jamieson, Optical Engineering, 25 (5), 688 (1986).

2) L.S. Yu, C.J. Berry, R.E. Drake, K. Li, R. Patt, M. Radparvar, S.R. Whiteley, and S.M. Faris, presented at the Applied Superconductivity Conference, Sept. 1986, Baltimore, MD. To be published in IEEE Trans. on. Mag..

3) C.S. Owen and D.J. Scalapino, Phys. Rev. Lett. 28, 1559 (1972).

4) J.H. Weaver, D.W. Lynch and C.G. Olson, Phys. Rev. B 7, 4311 (1973).

5) M. Radparvar, M.J. Berry, R.E. Drake, S.M. Faris, S.R. Whiteley, and L.S. Yu, presented at the Applied Superconductivity Conference, Sept. 1986, Baltimore, MD. To be published in IEEE Trans. on Mag..

TABLE I

Projected Comparision of HYPRES Josephson sensors
versus currently available sensors

Sensor	Responsivity	NEP (W)	Quantum Efficiency	Optical Bandwidth microns
GaAs Avalanche	200 A/W	$1*10^{-15}$	285.7	0.8 to 0.9
Si Avalanche photon counter (77K)	§10^{18} photons/W	$5*10^{-16}$	0.58	0.8 tested
Pyroelectric (300K)	5000 V/W	$2.9*10^{-10}$		8-14
Photomultiplier	0.04 A/W	$1*10^{-16}$		UV to 1um
GaInAs (300K)	3000 A/W	$1*10^{-15}$	0.56	1.2 to 1.7
Japanese Superconducting BPB detector	15000 V/W	$7*10^{-14}$		1 to 10
Present performance of HYPRES niobium junctions	10^4 to 10^5 V/W	$5*10^{-13}$	200 (at 1 um)	1 to 20
Ultimate performance of HYPRES niobium junctions	10^5 to 10^6 V/W	$1*10^{-16}$	960 (at 1 um)	Gamma ray to microwave

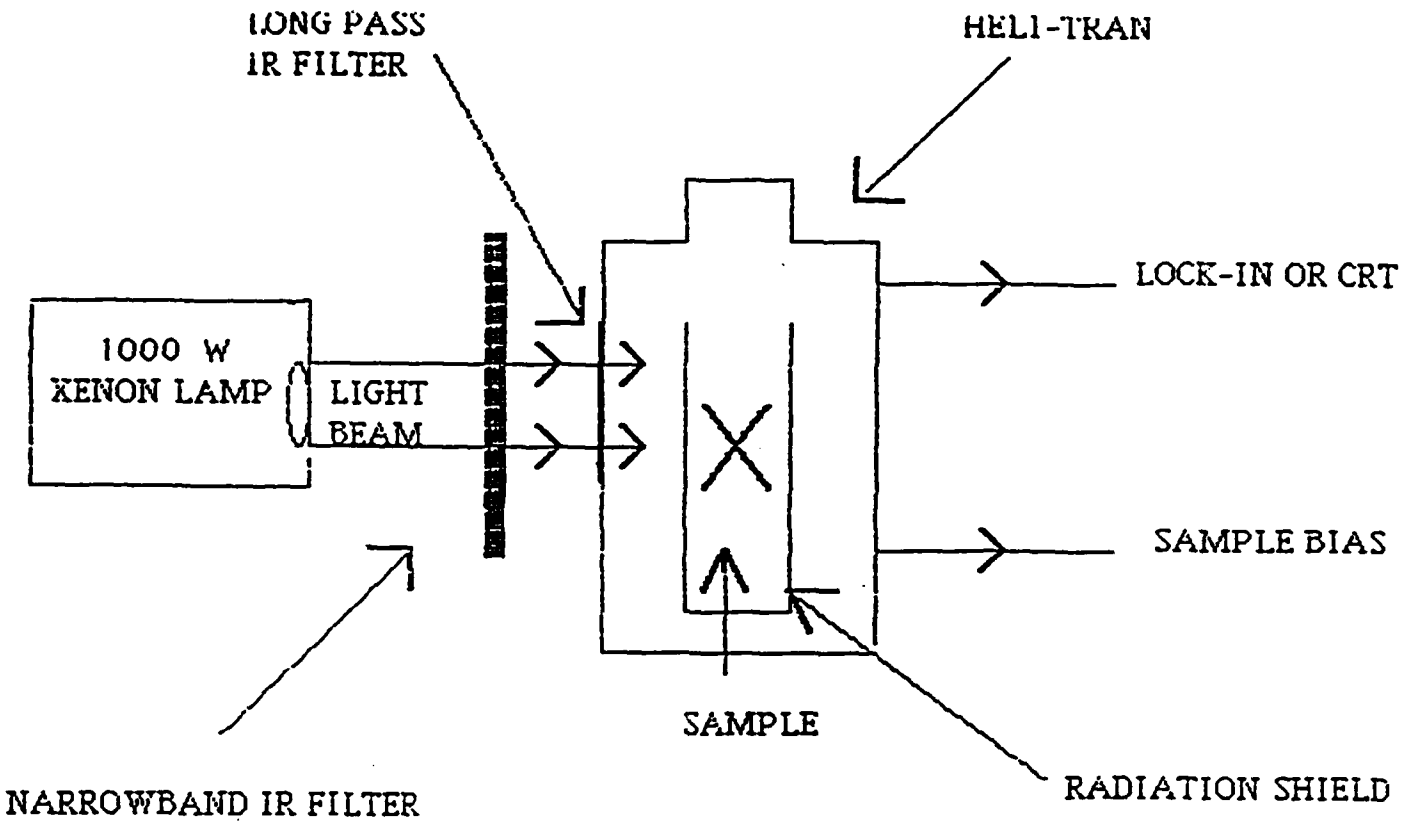

Fig. 1 Experimental arrangement for studying optical response of Josephson junctions and arrays to infrared radiation.

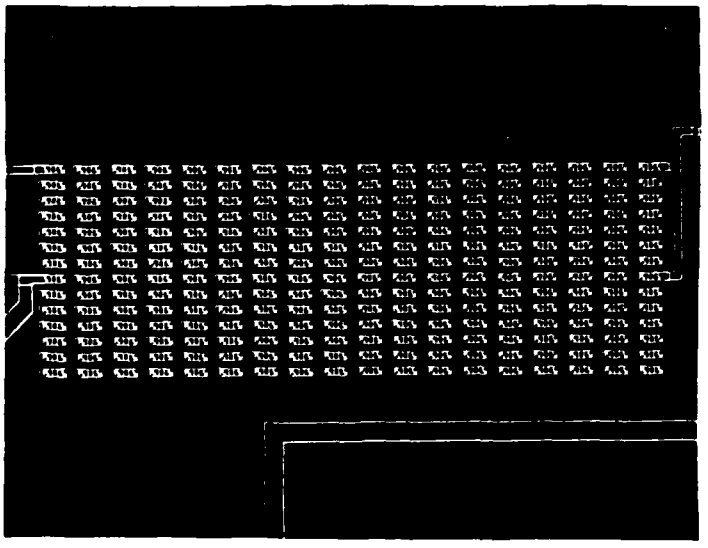

Fig. 2 A chain of 500 Nb-AlOx-Nb Josephson junctions used in the experiment.

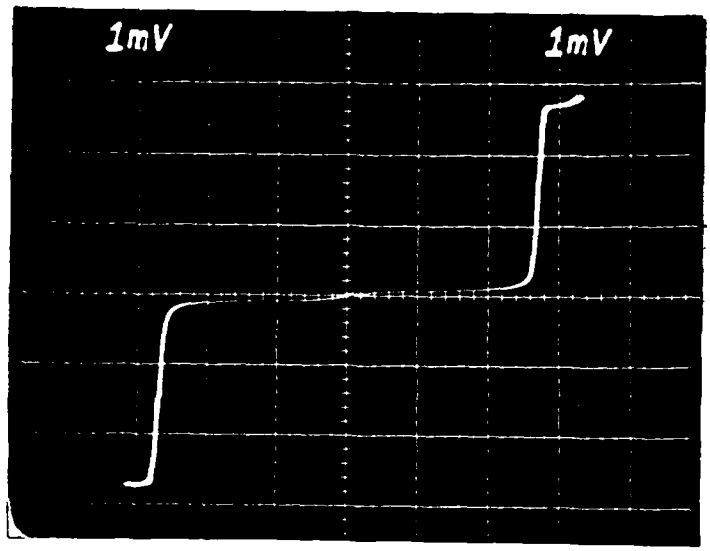

I = 0.2mA/div.

V = 1mV/div.

Fig. 3 The I-V characteristics of a Nb-AlOx-Nb Josephson junction at 4.2K.

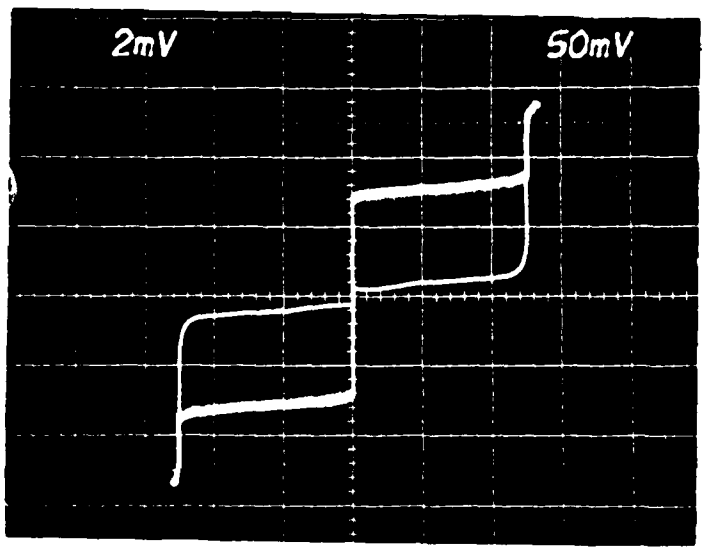

I = 0.2mA/div.

V = 50mV/div.

Fig. 4 The I-V characteristics of an array of Josephson junctions at 4.2K.

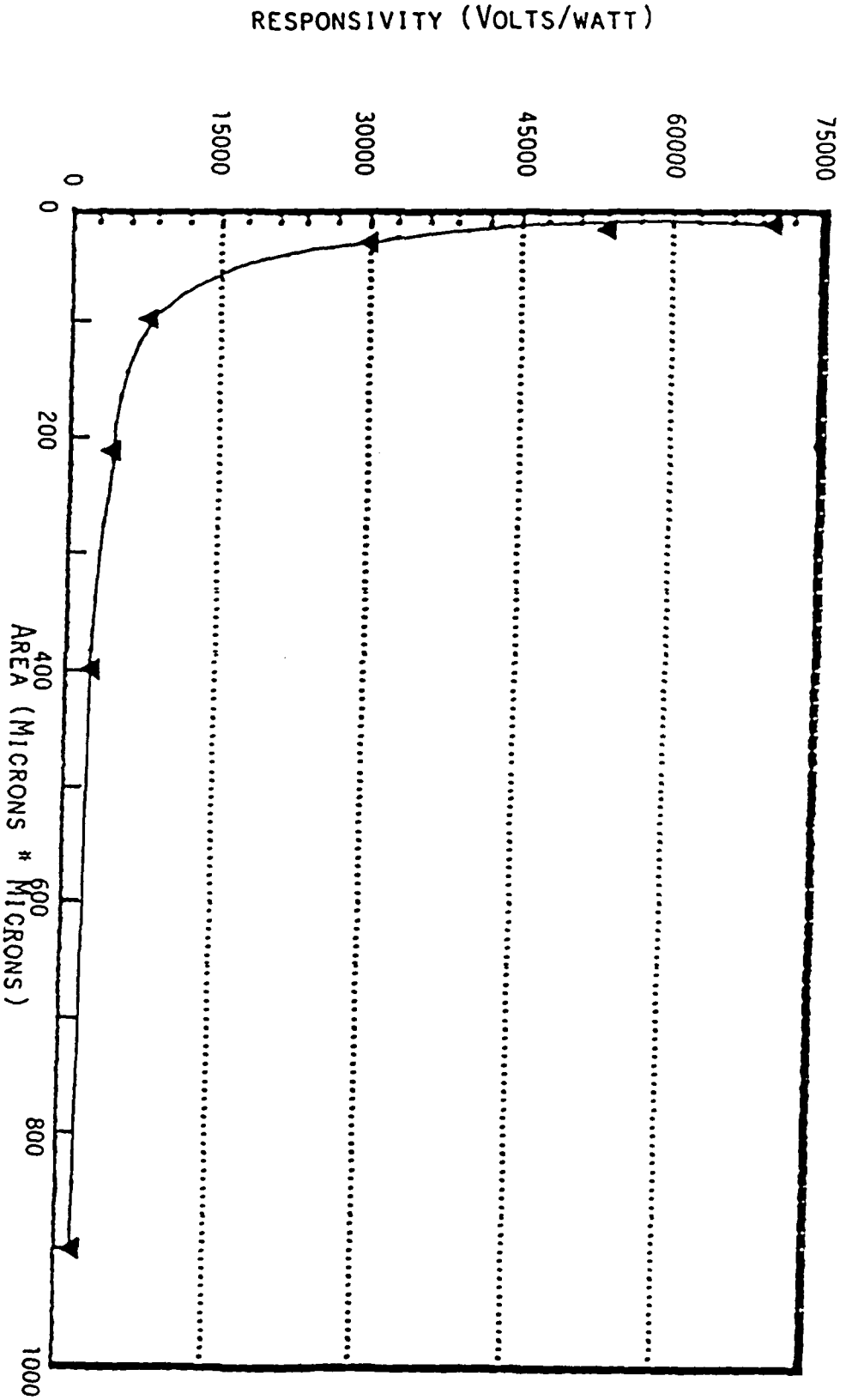

Fig. 5 Junction responsivity vs. area at 1 micron wavelength.

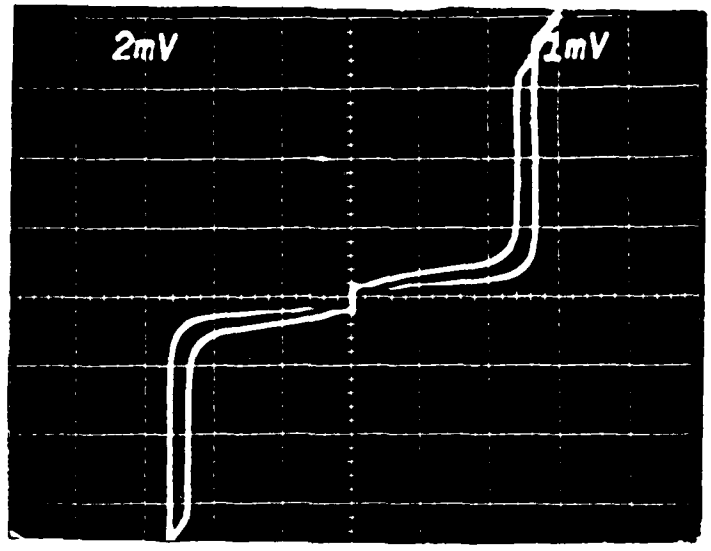

I = 0.2mA/div.

V = 1mV/div.

Fig. 6 The I-V characteristics of a Nb-A1Ox-Nb Josephson junction, without and with irradiation.

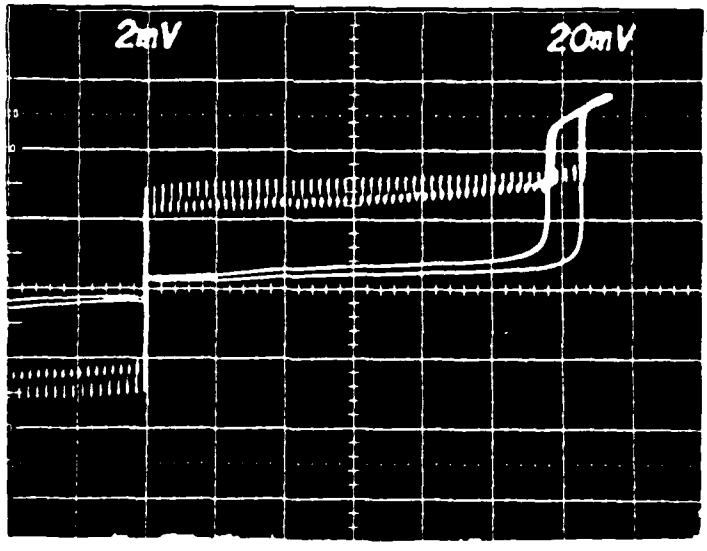

I = 0.1mA/div.

V = 20mV/div.

Fig. 7 The I-V characteristics of an array of 50 Josephson junctions, without and with irradiation.

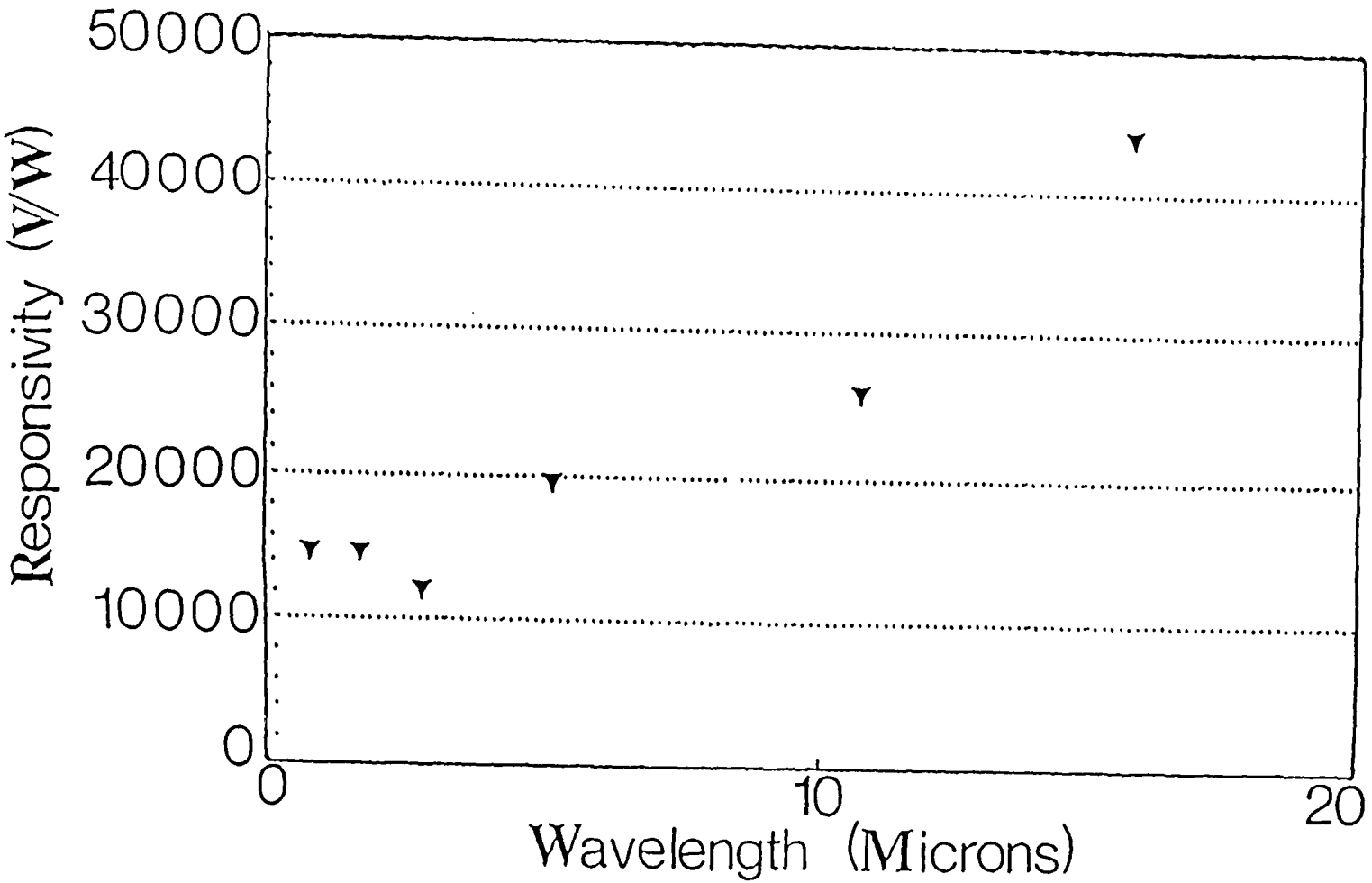

Fig. 8 Results showing ultra-high sensitivity of an array of junctions in the wavelength region 1 to 20 microns.

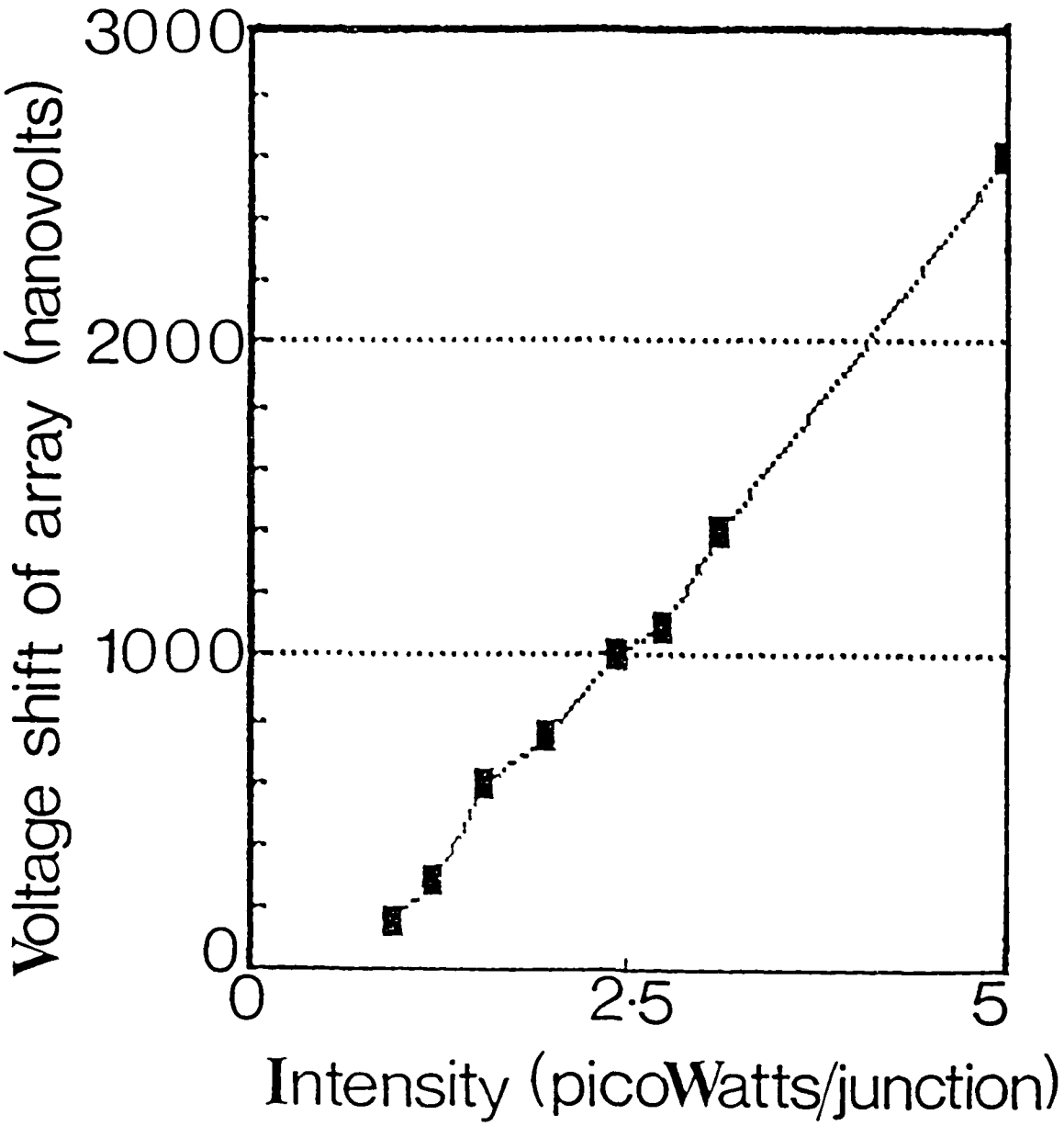

Fig. 9 Linearity of response of an array of 50 junctions, at ultra-low intensities. Lamp intensity calibration errors may be the cause for the line not passing through the origin.

END

3-87

DTIC